Fluxgate Magnetometer

6.101 Final Project Report

Massachusetts Institute of Technology
May 2016
Woojeong Elena Byun
Jack Erdozain
Farita Tasnim

Table of Contents

Abstract

Our goal for the 6.101 final project was to design and implement a fluxgate magnetometer, a high precision magnetic field sensor that consists of two coils and a magnetic core. The technology of fluxgate magnetometer was invented in 1936 in order to detect submarines; upon its invention, it helped prove the theory of plate tectonics. Now, it is widely used in both industry and academia thanks to its affordability, ruggedness, and compactness. It is also used in NASA's satellites because of its high sensitivity. Our team chose to construct a fluxgate magnetometer because it elegantly manipulates a physical concept to create a practical and precise sensor.

The core of the fluxgate magnetometer is driven by an AC current that saturates the magnetic core in a symmetric fashion about 0V. Any external magnetic field is sensed by the outer coil by causing changes in current which causes a DC offset proportional to the strength of the magnetic field. Through phase demodulation circuitry, we can extract the magnetic field signal.

Our final product demonstrated a one axis fluxgate magnetometer operation with core excitation driven by timing circuitry and current amplifiers, phase demodulation achieved through comparator circuitry and op-amp filtering and amplification, as well as ammeter functionality and the display of current through video and audio.

I. Introduction

A fluxgate magnetometer is a highly precise magnetic field sensor. Its typical sensitivity range is fit for measuring earth's magnetic fields, but it is also capable of resolving external magnetic field strengths less than .01% of that range. The core technology behind a fluxgate magnetometer was invented in 1936 before the Second World War with the goal of easily detecting submarines; upon its invention, its impressively high sensitivity helped prove the theory of plate tectonics by measuring shifts in magnetic patterns on the seafloor.

Fluxgate magnetometers are widely used in both industry and academia because they are affordable, rugged, and compact; they have been miniaturized to the point of IC sensor solutions with recent technology. The applications of a fluxgate magnetometer are many and varied: they can be used to observe small changes in the Earth's magnetic field for earthquake detection; their field

detection can be used to detect solar phenomena on earth; recently, NASA invented a magnetometer technology employing many fluxgates placed around a satellite in order to measure a combination of spacecraft-generated noise and magnetic field measurement data. Using subtractive algorithms, the two were separated for accurate magnetic field data collection. The low-power, compact, and inexpensive fluxgate no-boom solution has since been employed in NASA's CubeSat units.

The fluxgate elegantly manipulates a physical concept to create an extremely practical and precise sensor. The goal of this project was to design and construct a fluxgate magnetometer that demonstrates toroidal drive, signal processing with phase demodulation, and ammeter functionality with display.

II. Block Diagram

The fluxgate magnetometer is best described when divided up into five components. The timing circuitry drives the toroidal coil into positive and negative saturation with frequency f. The sense coil inherently picks up a signal proportional to any external magnetic field present. This signal is then extracted to a sine wave, of frequency 2f, magnitude corresponding to the strength of external magnetic field, and phase corresponding to the direction of external
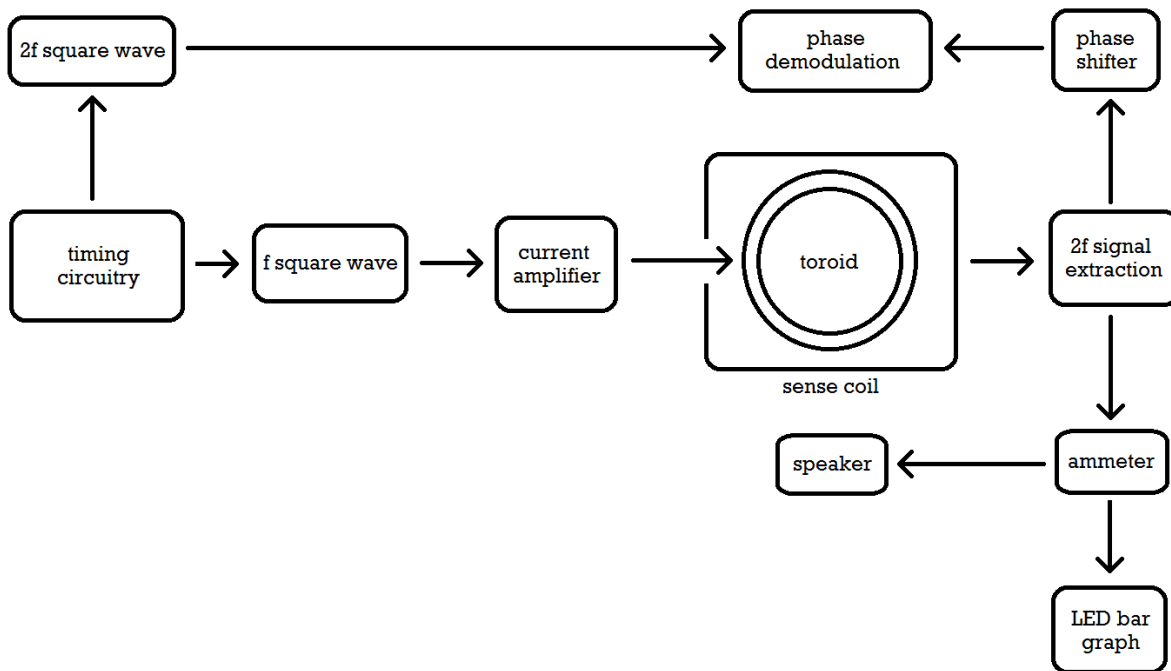

Figure 1. Fluxgate Magnetometer High Level Block Diagram

magnetic field. This extracted 2f sine wave signal then feeds into two different blocks: (1) phase demodulation to extract a DC voltage output that demonstrates magnitude and directionality of magnetic field and (2) an ammeter with display for magnitude and directionality of current with LED's and a speaker. Figure 1 depicts a high-level block diagram of the system. Figure 3 depicts a low-level block diagram of the fluxgate magnetometer that will be used to explain each system in further detail.

III. Design Overview

A. Toroid and Sense Coil Construction

The goal of the drive and sense coils was to achieve a means by which (1) a core can be driven to saturation in order to gate flux and (2) a sense coil can then detect a signal of double the drive frequency, with amplitude proportional to the external field.
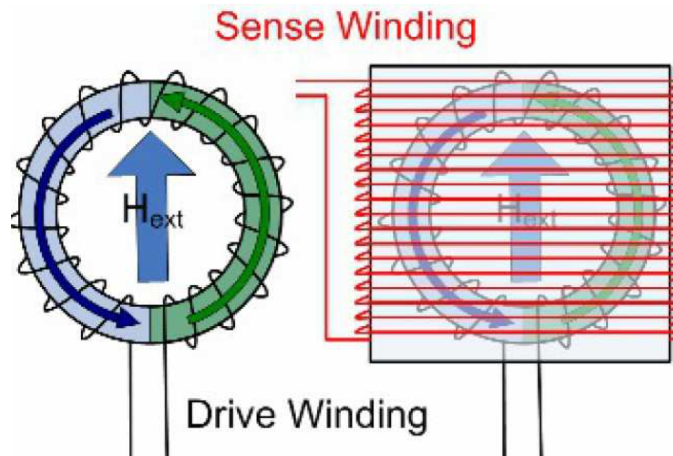

Figure 2. Sense and Drive Coil Depiction[1]

A rod core can be used as the drive core, but as the magnetic fields from saturation would not a cancel in a rod, a toroidal core is preferred, as used in this system. The symmetry of the toroid ensures that any magnetic field induced on the right side is cancelled on the left and vice versa. The sense coil is placed around the toroid for external field detection, and due to the cancelling effects of the toroid's symmetry, can only sense signals resulting from external magnetic field. The sense coil in this system uses a turn count of about 500 turns of 38 gauge magnet wire. A depiction is shown in Figure 2.
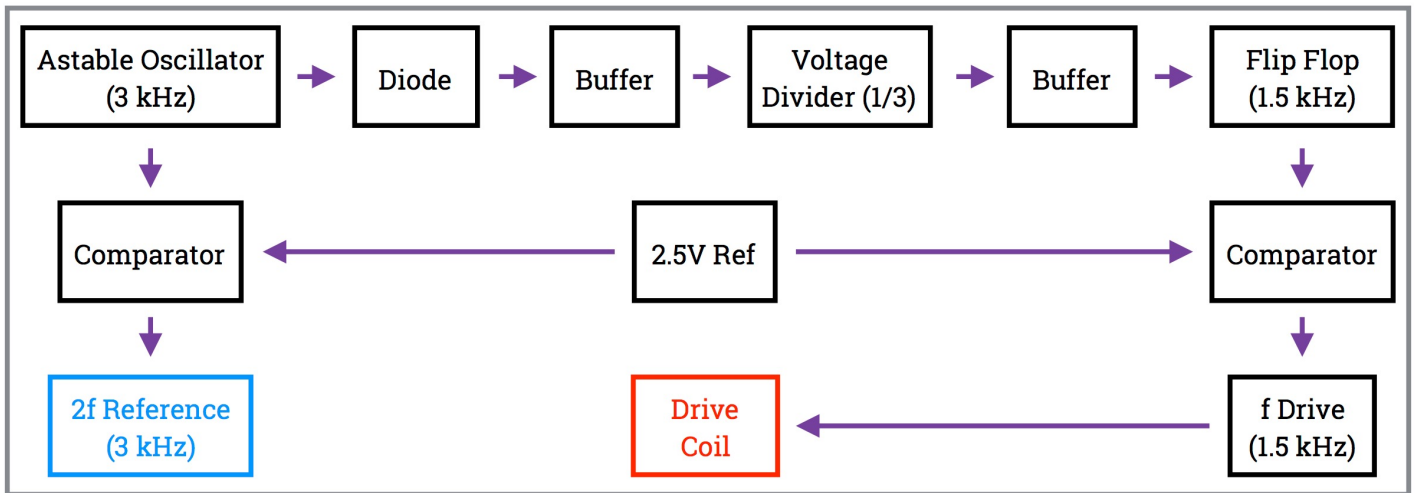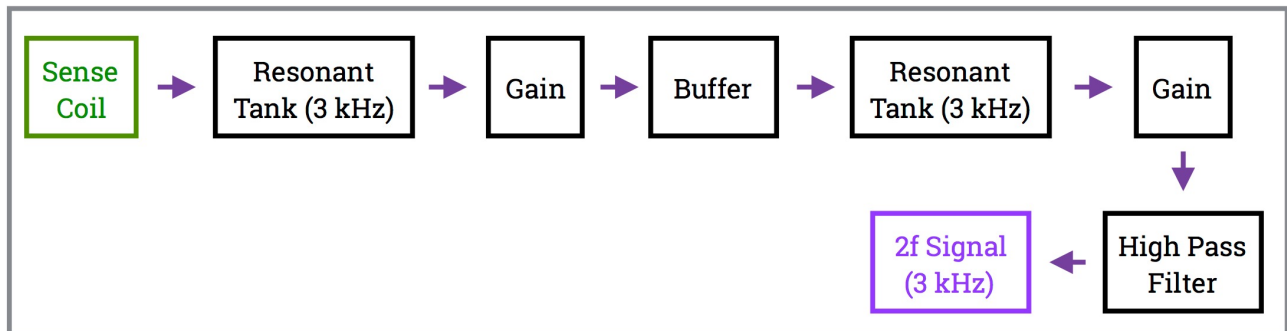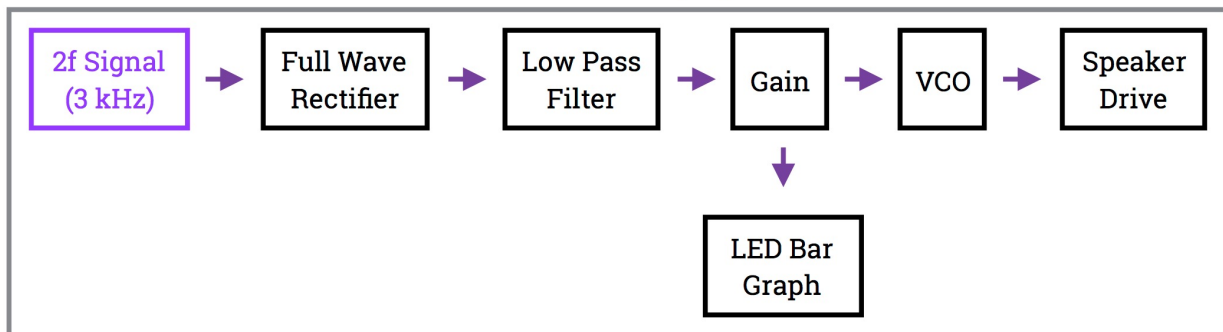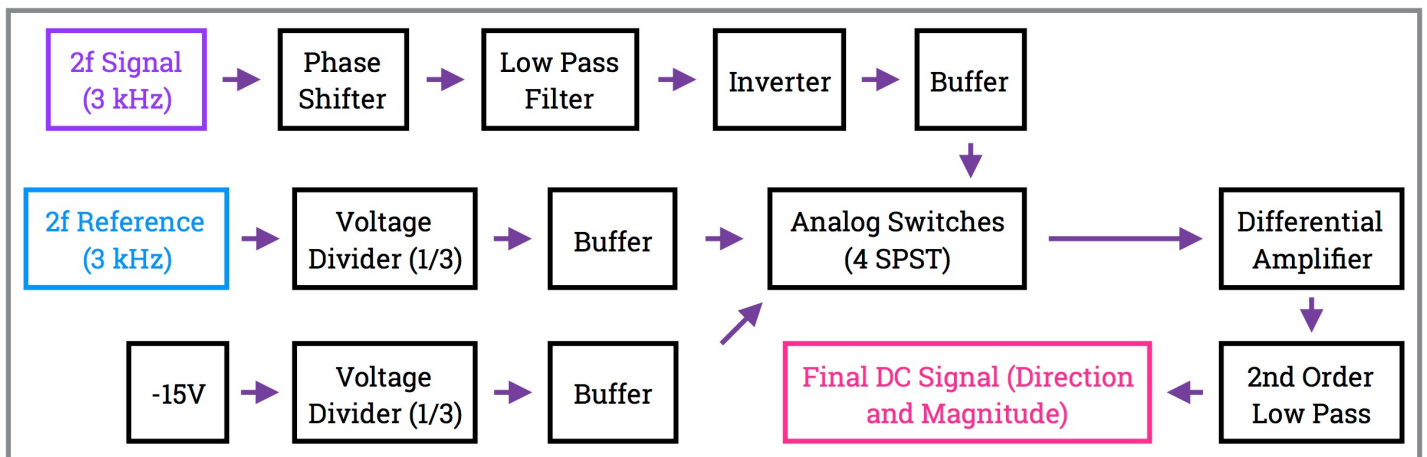
Figure 3. Fluxgate Magnetometer Low Level Block Diagram

The drive coil operates as the means by which the system gates flux, which involved driving the core into saturation, up to 100 times the initial saturation point, and then into saturation in the reverse direction. Saturation was best achieved with an AC-coupled square wave signal to be driven across the toroidal core. At saturation, the magnetic field inside the toroidal core collapses, and thus its inductance drops to zero. This phenomenon of completely ridding the toroid of magnetic field is exactly what allows for the sense coil to achieve highly precise detection of external magnetic fields. It was critical, therefore, to determine the proper number of turns at our chosen drive frequency of 1.5 kHz so that the system would operate in saturation.

The number of turns around the drive coil was determined experimentally. The current needed to saturate the core is proportional to the number of turns. For this reason, a lower number of turns around the toroid is preferred. One toroid was wrapped with 150 turns of 32 gauge magnet wire; however, the resulting inductance was approximately 1 H, which was far too difficult to saturate with our drive circuitry. Amps of current would have been needed to drive that core into saturation. Instead of building power-heavy drive circuitry, the number of turns around the toroid was divided by a factor of 1/4 to become 56 turns, and thus the inductance went down by a factor of 16 to become approximately 55 mH. This final toroidal core was able to reach saturation with approximately 50 mA of AC current.

The permeability of the core is also extremely important to achieving saturation with lower levels of current. The saturation current required is inversely proportional to the permeability. For this reason, a metallic glass core, specifically MODEL HERE was used, as its relative permeability of 20,000 is fairly high, especially in comparison with ferrite cores whose relative permeability is on the order of 600.

B. Timing and Toroidal Drive

In order to achieve proper functionality of the fluxgate magnetometer, the drive coil had to be driven into saturation. Figure 4 depicts the entire schematic for timing circuitry and toroidal drive. Timing and drive involved creating square waves at frequency f (1.5 kHz) and 2f (3 kHz) as well as amplifying the 1.5 kHz signal in order to drive the toroidal core into positive and negative saturation.
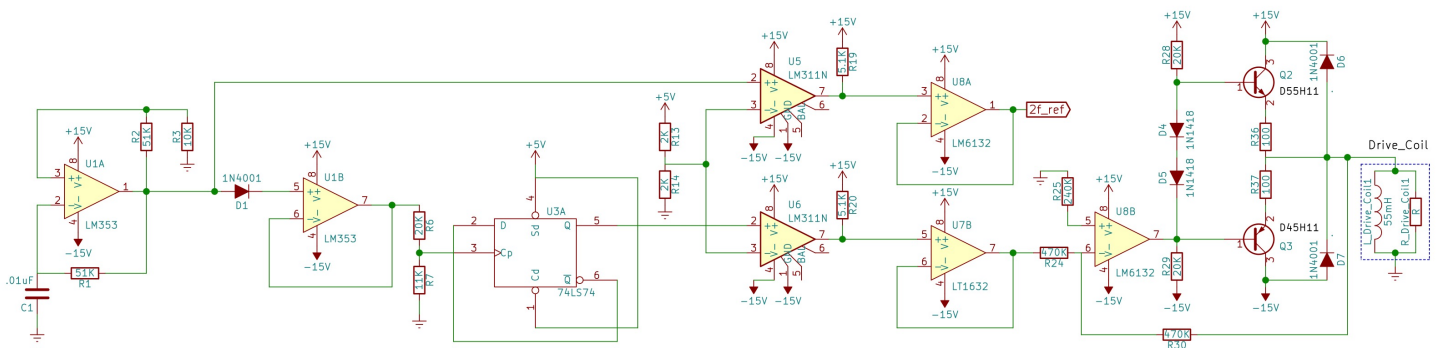
Figure 4. Full Schematic for Timing and Toroidal Drive

The 3 kHz signal was created first and then halved with a flip flop because it is easier to half a frequency and maintain a 50% duty cycle than to double a frequency while maintaining duty cycle. The 3 kHz signal was generated using an LM353 in astable oscillator configuration, as shown in Figure 5. The formulas for calculating the frequency of operation of an astable oscillator are:

$$\beta = R_3/(R_2 + R_3)$$
$$T = 2(R_1)(C_1)*\ln((1+\beta)/(1-\beta))$$
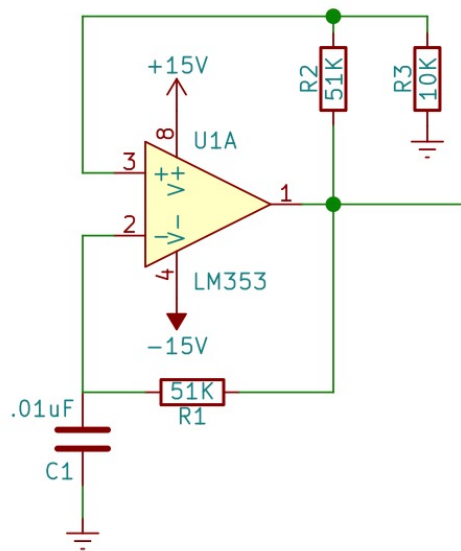$$f = 1/T$$

Figure 5. Astable Oscillator

Values for resistors and capacitors were chosen to achieve a square wave output with frequency 3 kHz. The output of the astable oscillator was then fed into both the halving circuitry and reference signal generating circuitry.

For phase demodulation, a reference signal at the 2f frequency, which is 3 kHz, is needed in order to properly determine the phase of the sense coil signal also present at frequency 2f. To generate this 2f frequency with higher current capability in order to drive analog switches, a comparator and buffer were used, as shown in Figure 6. The comparator compared the astable oscillator output to a 2.5V DC voltage level and produced a 2f square wave that was then fed into a buffer that prevented current draw from later stages from affecting the 2f reference signal.
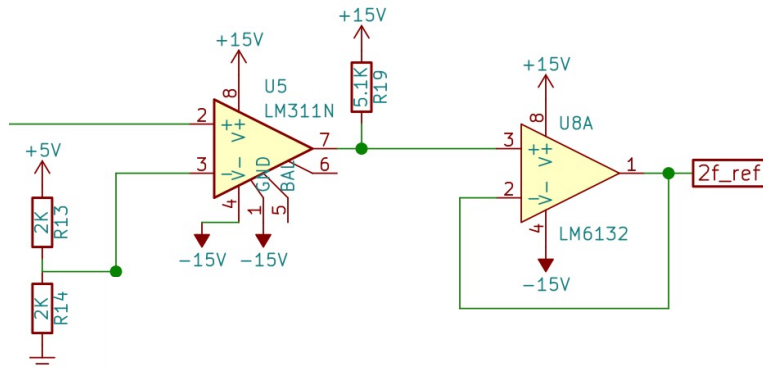

Figure 6. Comparator and Buffer 2f Reference Signal Production

Finally, a square wave of frequency f, or 1.5 kHz, which can source about 50 mA, was produced to drive the toroidal core into saturation. First, the 2f frequency was halved using a flip flop. Since the output of the astable oscillator is a square wave that operates from +15V to -15V, and the flip flop only operates from 0V and 5V, a couple stages were added to achieve voltage level conversion, as seen in Figure 7. A diode and buffer were used to get +15V to 0V operation, after which the signal was fed into a voltage divider to achieve +5V to 0V operation. The +5V to 0V square wave at frequency 2f is then fed into a D-flip flop configured such that the D input is tied to the Q-bar output. This way, the output of the flip flop is a +5V to 0V square wave at frequency half of 2f: f, or 1.5 kHz.
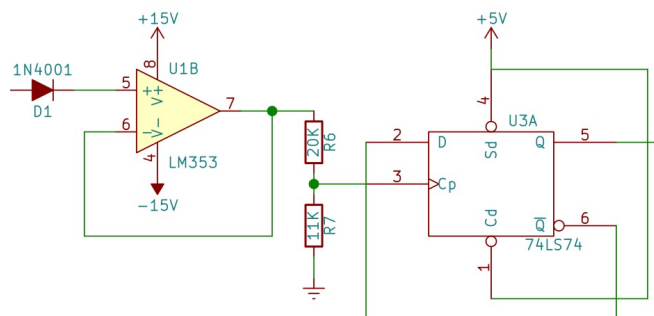

Figure 7. 1.5 kHz Signal Generation

9

The square wave output of the flip flop was then converted back into +15V and -15V levels, since the core is supposed to be driven into positive and negative saturation. The positive and negative square wave is then fed into a buffer and amplification stage, as depicted in Figure 8. The amplification stage is a class AB amplifier, or push-pull amplifier, with feedback to remove any distortions introduced by crossover distortion. The final output went straight into the toroidal drive coil.
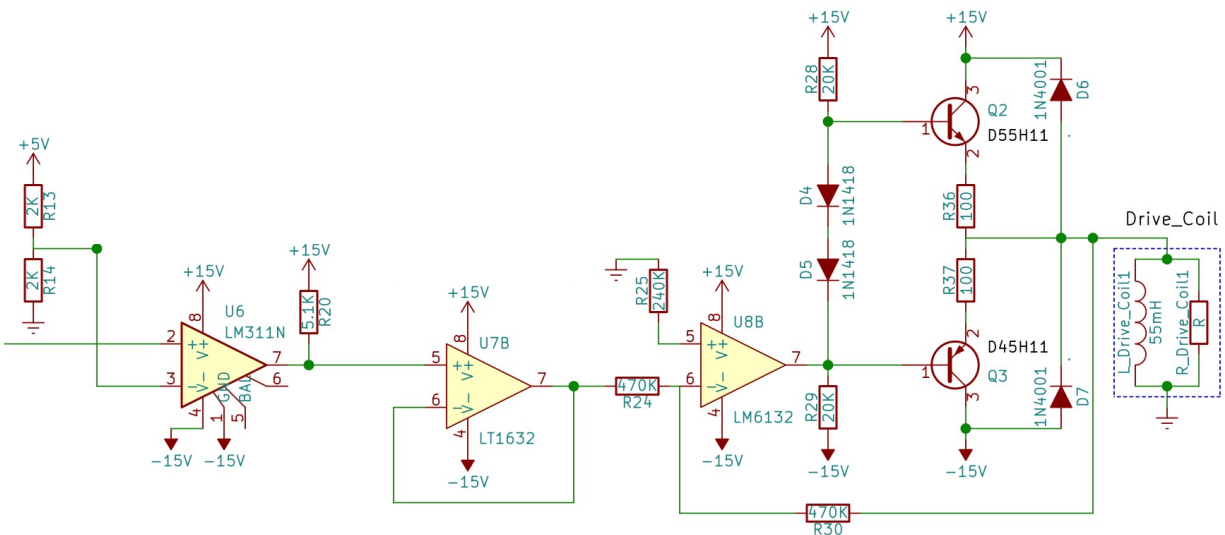

Figure 8. 1.5 kHz Signal Amplification for Toroidal Drive

Since the drive coil was made of metallic glass, its relative permeability was very high: on the order of 20,000. Thus, it was much easier to drive into saturation than a ferrite core. The drive coil needed a current on the order of 50 mA. This current was determined experimentally. A couple of different strategies for current amplification were tested, including a simple buffer and a class B amplifier, but the best strategy turned out to be a simple push-pull amplifier with feedback. The output waveform across the drive coil is shown in Figure 9 (yellow). When the square wave collapses for some time on both the positive and negative half cycles of the square wave, the core is driven into saturation. This collapse occurs because, when driven into saturation, the permeability of the toroidal core goes to essentially zero, as does the inductance. When saturation happens, the core can be modeled as a resistor in parallel with a negligible parasitic capacitance. Since this resistance is small even when compared to the resistance of the drive signal output from the push-pull amplifier, the voltage essentially drops to 0V. Then, when the core is driven in the opposite direction, the

inductance returns until the toroid again reaches saturation, when the square wave again collapses.
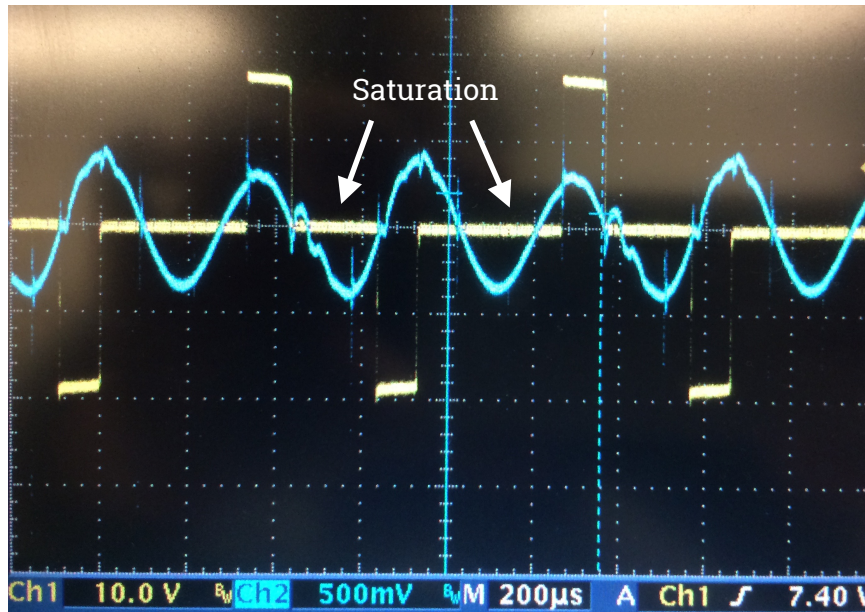

Figure 9. Waveform Across the Toroidal Drive Coil (yellow)

C. Sense Signal Extraction

In order to find the magnitude and polarity of the external magnetic field, the 2f frequency component must be extracted from the sense coil response. In order to isolate the 2f signal only, two LC resonant tanks were employed, as shown in Figure 10.
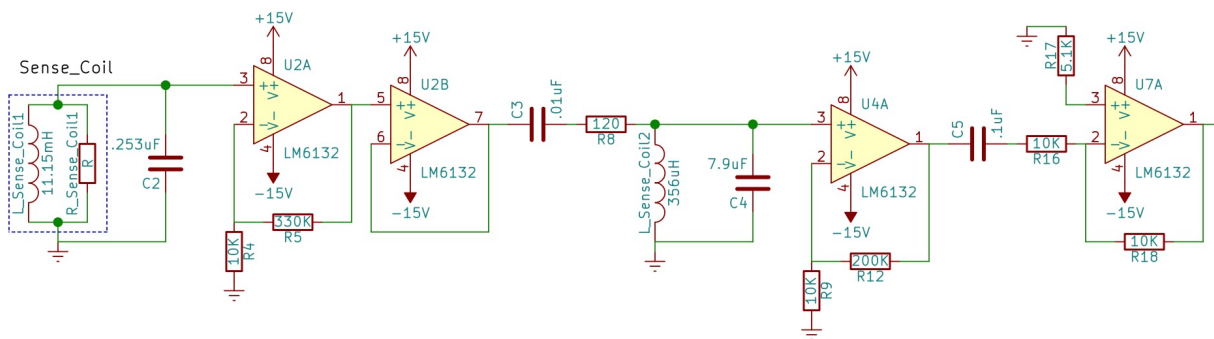

Figure 10. Sense Signal Extraction

The resonant frequency and Q of a parallel LC tank can be found through the following equation:

$$f = 1/(2\pi * \sqrt{(LC)}); Q = 2\pi f RC$$

11

The first LC tank used the sense coil as the resonant inductor and a capacitance tuned to produce a resonant frequency of approximately 2f. It was discovered that the inductance of the sense coil was susceptible to much variance. Slight changes made to the shape of the coil or the placement of the toroid inside of it could change or resonant frequency very easily. Therefore, the first tank was built with a generous Q, high enough to cut out most of the unwanted frequencies, but low enough to make sure that we would not accidentally lose our critical data in the 2f signal.

In order to fully attenuate the first and third harmonics successfully, however, a high Q circuit was desirable. Therefore, after a gain step to amplify our small signal and a buffering step, another LC tank with a known and fixed inductor value was constructed, as shown in Figure C. This tank was tuned to precisely the 2f frequency, and the resistor value was chosen for a small bandwidth such that the magnitude rolled off significantly enough at the first and third harmonics.

Following another gain stage, a high pass filter was added in order to eliminate any DC offset that was introduced to the signal due to the tanks. At the output of the high pass is a very clean 2f sine wave with amplitude proportional to the magnitude of the magnetic field and phase corresponding to the direction of the magnetic field. This signal is now ready to enter the phase demodulation block as well as the ammeter display circuit.

D. Phase Demodulation

In order to extract the directionality and magnitude of external magnetic field, a phase demodulator was employed. Phase demodulation means displaying the degree to which the 2f signal from the sense coil is out of phase with the drive frequency with a DC voltage. With magnetic field, direction and magnitude are inherently linked because, the magnitude of the external magnetic field parallel to the direction that the sense coil detects field changes as the external magnetic field changes direction. When magnetic field flips, however, the 2f sense coil signal flips, which is equivalent to a 180 degree phase shift. Normal magnitude detection of magnetic field would not account for this reversal of direction; however, with phase demodulation, the DC output voltage becomes negative when the direction of the magnetic field reverses. To illustrate, Figure 11 shows a graph of the expected relative DC voltage level with changing phase angle.
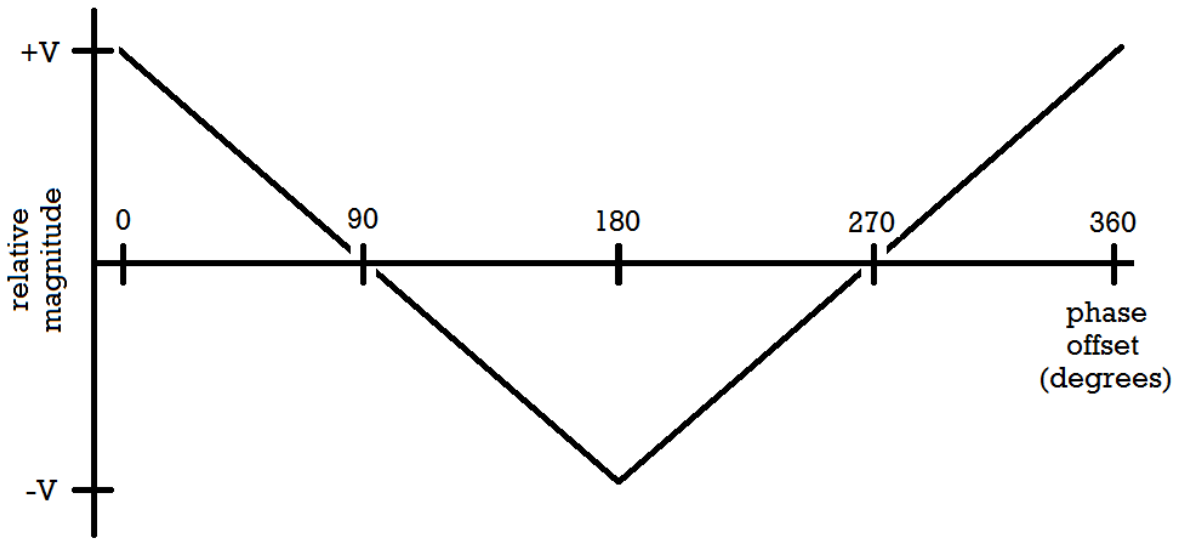
Figure 11. Graph of Expected DC Output Demonstrating Phase Shift for Directionality
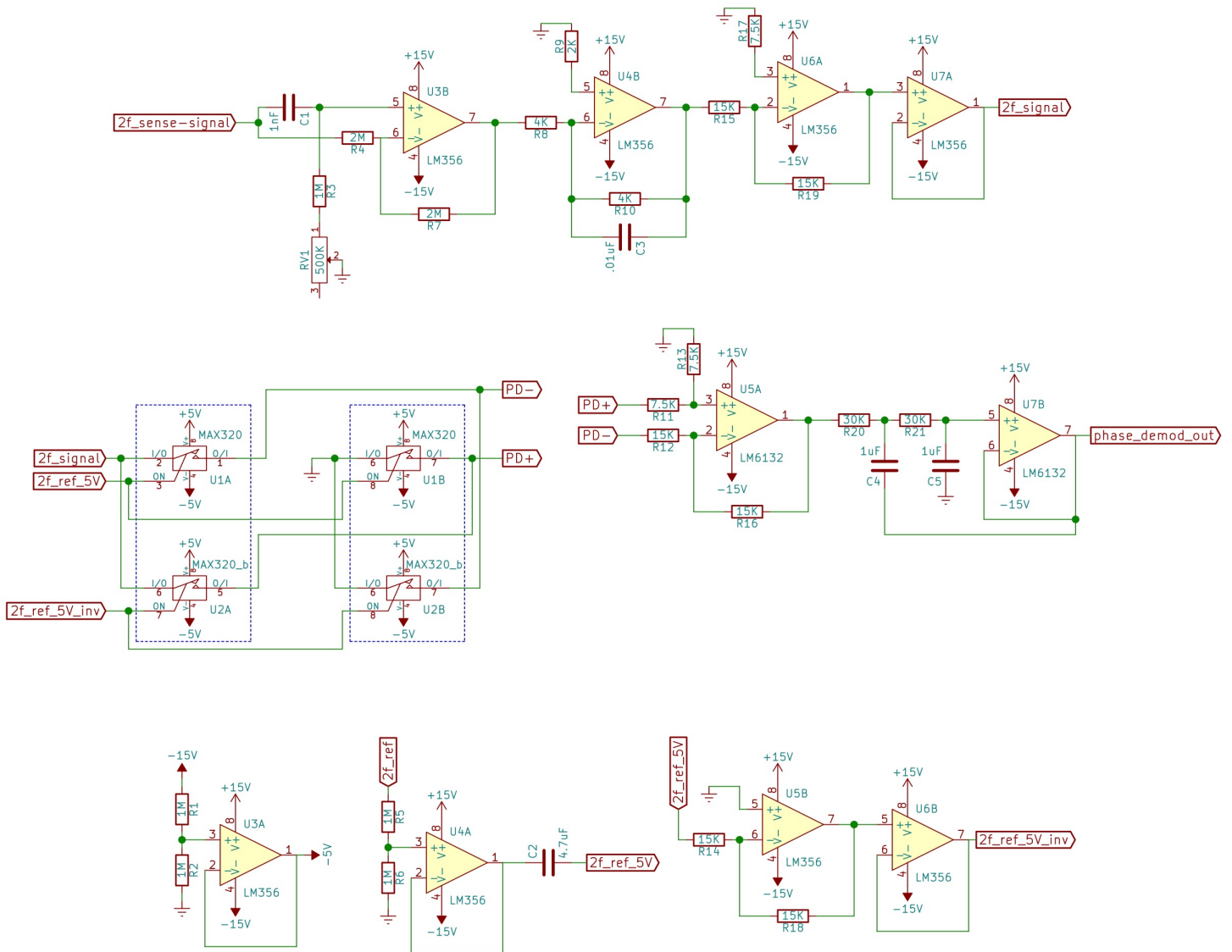

Figure 12. Full Schematic for Phase Demodulation

13

The full circuit for phase demodulation is shown in Figure 12. The phase demodulator can be broken up into three parts: 2f sense coil signal phase shifter, 2f reference square wave voltage conversion and inversion, and synchronous detection.

Due to inherent delays in the circuitry as well as response time delays between the toroidal drive and the sense coil pickup, the desired 2f sense coil signal is phase delayed from the actual drive signal. A phase shifter was built, as shown in Figure 13, to phase shift the 2f sense sine wave to be completely in phase with the 2f reference signal generated by the timing circuitry, which is also in phase with the drive frequency. The phase shifter was calibrated by (1) using a bidirectional test magnet placed at a fixed distance and turned such that the greatest possible magnetic field was completely in parallel with the detection direction of the sense coil and (2) aligning the 2f sine wave output resulting from the placement of this magnet such that the zero crossing point of the sine wave matches up with the zero crossing of point of the 2f reference square wave.
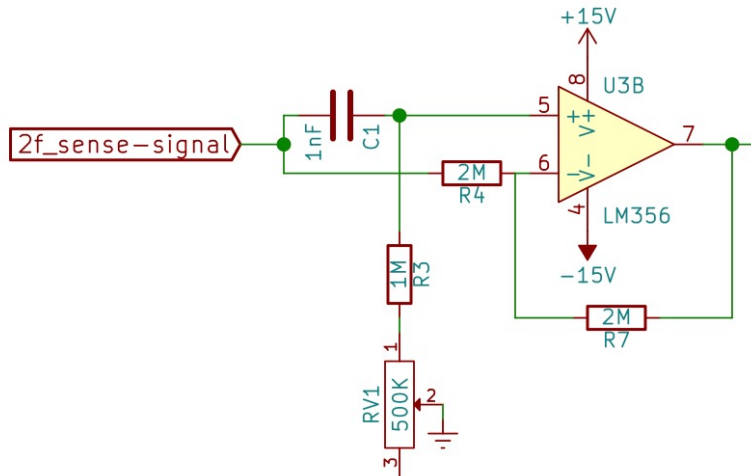

Figure 13. Phase Shifter

After testing, it was determined that the 2f signal in the positive direction was out of phase from the 2f reference square wave, and thus the drive frequency, by approximately 43 degrees. The phase shifter was built as an all-pass filter that phase shifted its input within the range of 40 degrees to 50 degrees based on the value of a potentiometer. The equations for determining the phase shift that can be achieved from this phase shifter[2] are:

$$V_o/V_{in} = (s - 1/RC)/(s + 1/RC)$$
$$\text{phase shift} = -2*\arctan[RC/(2\pi f)]$$

After the 2f sense signal was shifted to align with the drive waveform, it was fed through an inverting active high pass filter with cutoff at approximately 600 Hz to get rid of DC offset, followed by an inverting amplifier with unity gain to undo the signal inversion, and finally a buffer to prevent current draw in later stages from affecting the extracted signal. These stages are depicted in Figure 14.
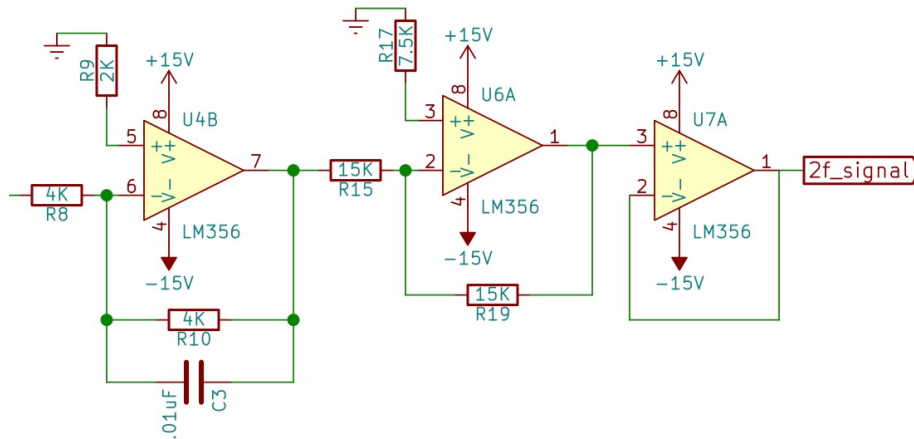

Figure 14. Removal of DC Offset and Buffering of 2f Sense Signal

In order for this particular design for phase demodulation to work, an inverted 2f reference was needed in addition to the original 2f reference square wave. These two square waves were also converted to +5V and -5V voltage levels were used to drive the analog switches responsible for chopping up the 2f sense coil signal. The circuitry to achieve this is shown in Figure 15. First, the 2f square wave reference was fed through a voltage divider and a buffer to achieve voltage conversion. Then, this +-5V square wave was fed through an inverting amplifier and a buffer to achieve the inverted 2f square wave reference. Also depicted, on the left with the voltage divider and buffer, is the generation of -5V line from -15V in order to be able to power the analog switches from the appropriate +5V and -5V.
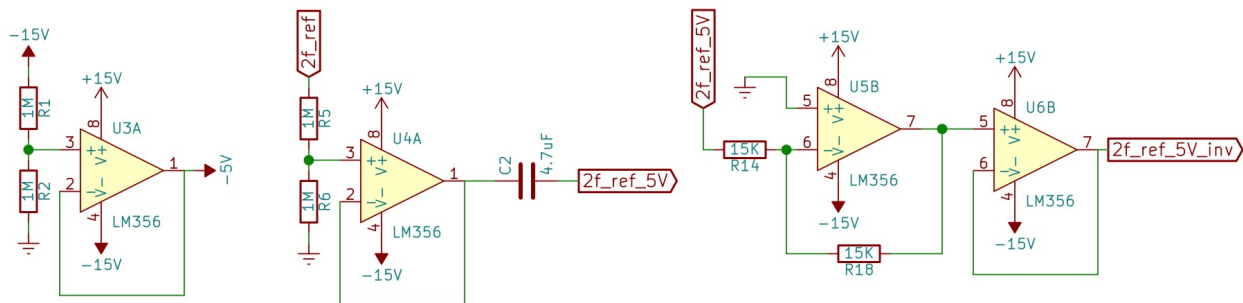

Figure 15. Readying Drive Signals for Analog Switches

Finally, our generated 2f sense sine signal and 2f reference square wave signals were fed into the synchronous detector. The first portion of the synchronous detector is a series of 4 SPST analog switches configured to act like two SPDT analog switches, as shown in Figure 17. The purpose of these switches is to split the 2f sense sine signal into two different signals: one that is in phase with the positive half cycles of the normal 2f reference square wave and one that is in phase with the positive half cycles of the inverted 2f reference. This is essentially like chopping the 2f signal at each edge of the 2f square wave. Figure 16 demonstrates the effect of the analog switches.
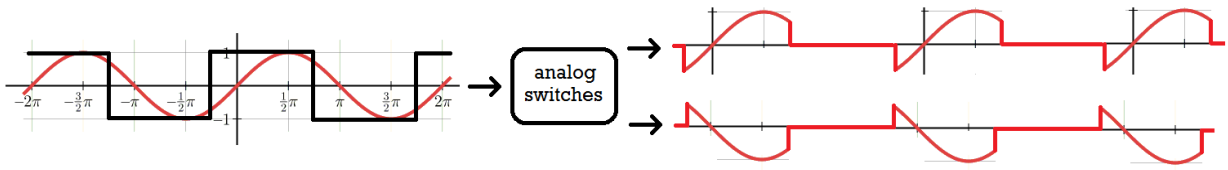

Figure 16. Input and Output of Analog Switches, Chopping of 2f Sense Signal

The MAX320 analog switches were chosen due to their very low charge injection (2-5 pC), low on-resistance (16 Ω), and fast switching speed (35-65 ns) which are important in order to preserve the integrity of the 2f sense signal even when chopping it up, as well as to be able to respond quickly to the fast-switching 2f reference square waves.
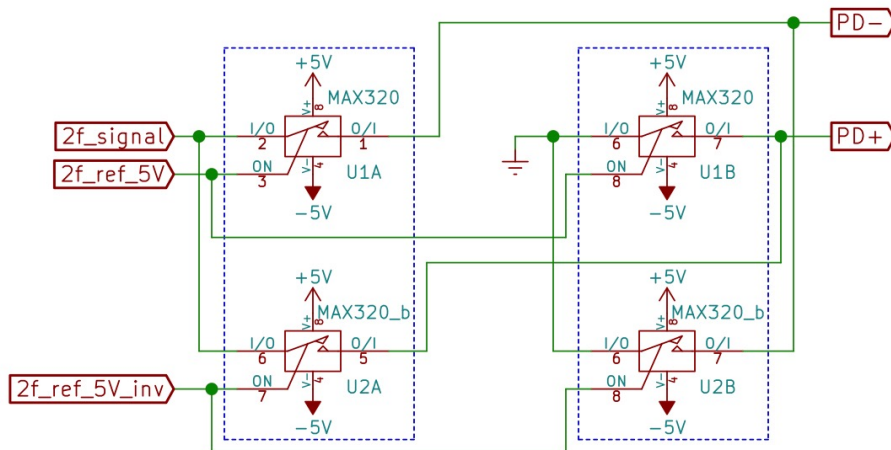

Figure 17. Analog Switch Circuitry

The two parts of the chopped up 2f sense signal are then fed into a differential amplifier and a second order active low pass filter in order to extract the final DC voltage output that displays magnitude and directionality of magnetic field. Figure 18 shows the diff-amp and the low pass filter. The differential amplifier basically acts like a subtractor here, according to the following equation:

$$V_{out} = (PD+)*R_{13}*(R_{12}+R_{16})/(R_{12}*(R_{13}+R_{11})) - (PD-)*(R_{16}/R_{12})$$

With the values given in Figure 16,

$$V_{out} = (PD+) - (PD-)$$

The second order low pass filter was chosen to extract only the DC differential output voltage. The cutoff frequency was set to X. The final signal after phase demodulation should be a DC voltage level that reverses sign when magnitude is flipped.
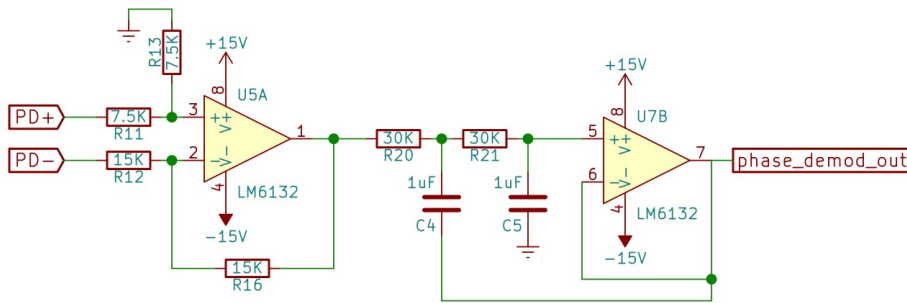

Figure 18. Differential Amplifier and Second-Order Low Pass Filter

To test proper behavior such that the output follows the graph in Figure 9, a magnet was placed at a fixed distance away from the sense coil. First, the magnetic field was oriented such that it was completely parallel to the sense coil detection direction. A positive or negative DC voltage was observed. Then, the magnet was slowly rotated. The output slowly tended towards 0V, and when the magnet was oriented such that the magnetic field was completely perpendicular to the sense coil detection direction, the output was 0V. The magnet continued to be rotated in the same direction. The output then reversed sign and kept increasing in magnitude until the magnet was rotated a full 180 degrees, at which point the same DC voltage that was observed at 0 degrees should be present, but with the opposite sign. Continued rotation in the same direction resulted in the output DC voltage to again go to 0V at 270 degrees, and finally back to the original DC output voltage at 360 degrees.

E. Ammeter and Display

Fluxgate magnetometers are an industry standard for use in non-contact current sensing applications because of their extreme accuracy robust design.

The goal of the ammeter display was to create audio and visual feedback that indicates the current flowing through a wire placed in the center hole of the toroidal core of the fluxgate magnetometer.

To display this information, an LED bar graph was built to increment a step , or turn on another LED, every time the input current increases by .1 A, with a range from 0A to 1A. This resulted in a total of 10 LEDs. Simultaneously, the display drove a speaker with a frequency proportional to the current in the wire as a means of audio feedback.
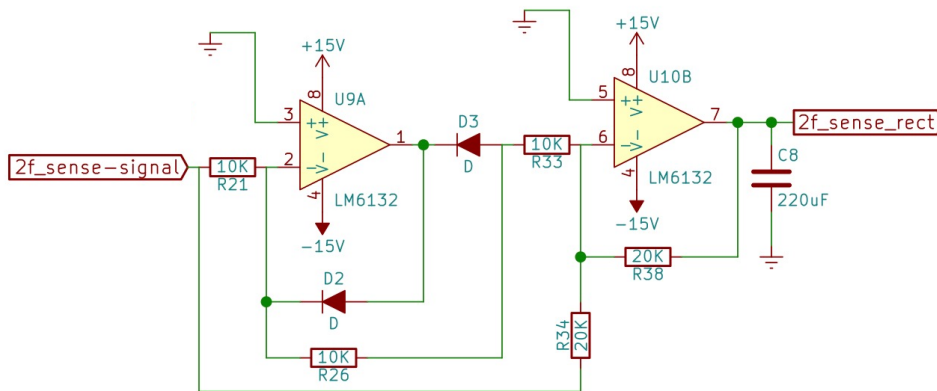

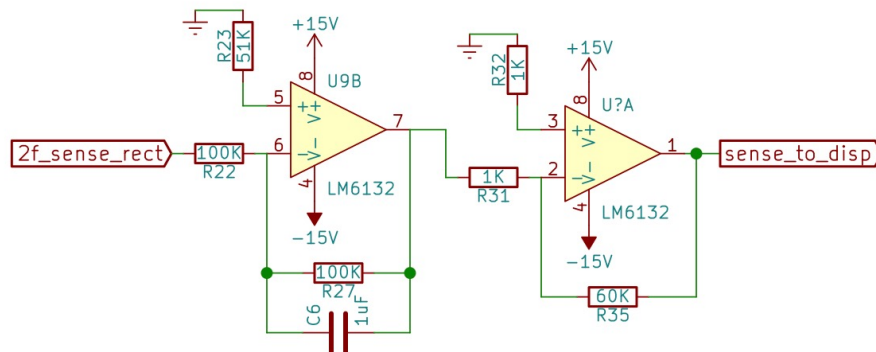Figure 19. Rectification of Sense Signal

Figure 20. Rectified Sense Signal Low Pass Filter and Amplification

In order to show the magnitude of the current, and thus the magnitude of the induced magnetic field, a precision full wave rectifier was employed to extract the amplitude data, as shown in Figures 19 and 20. The phase data is separately processed in the demodulation block to analyze the polarity of the current. The full wave rectifier output is then fed into an amplification step.

After the magnitude of the 2f sense signal was extracted, it was sent into the ammeter display stages. The amplification stage, as shown in Figure 21, included a non-inverting amplifier with an adjustable gain via a potentiometer. This signal gain was adjusted and calibrated to ensure that a wire carrying 1A produced a signal of 10V, while 0A produced a signal of 0V. This output then entered a non-inverting summation circuit which added a constant offset to the signal from a reference voltage provided by another potentiometer. The output of the summation circuit was then fed to an operational amplifier that had an N channel MOSFET in its feedback loop as a signal buffer. The output of this op-amp
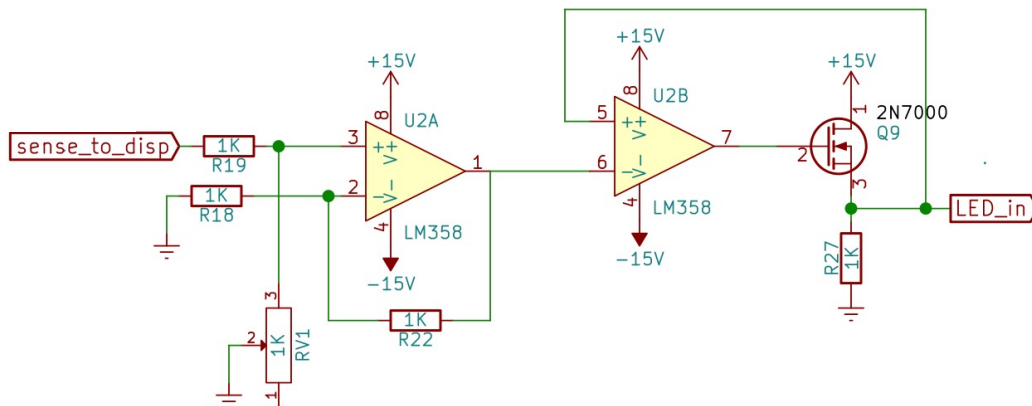

Figure 21. Creation of LED Drive Signal for Ammeter Display

then drove 10 separate diode-resistor dividers all in parallel. The diodes were each adjusted to produce 10 different forward voltages, each a single volt apart. When the voltage across each respective diode passed its forward voltage, the output of the diode resistor pair was pulled high, activating a low side MOSFET driver attached to an LED. The result was that at every incrementing rise of 1 volt on the input a new LED turned on. The purpose of the aforementioned summing circuit was to add an offset voltage equal to that of the 2N7000 MOSFETS used to drive the LED's. This ensured that the first LED turned fully on at around 1V instead of 1V plus the gate threshold voltage of the transistor. The problem is then that the diode-resistor blocks pull a good deal of current, beyond that of the operational amplifier's capabilities and therefore a MOSFET buffer stage was used to drive the chain.

There are a few advantages of this design over the use of comparators and reference voltages to activate the LEDs. One advantage is that this design is in part more scalable, more LEDs just means additional diodes, resistors and MOSFET's instead of adding more pricey ICs. Similarly, this design is better for size-constrained systems as a diode and resistor serve the purpose of an entire IC

and multiple voltage dividers (neglecting the additional MOSFET which would be needed in both cases to drive more power costly LED's).
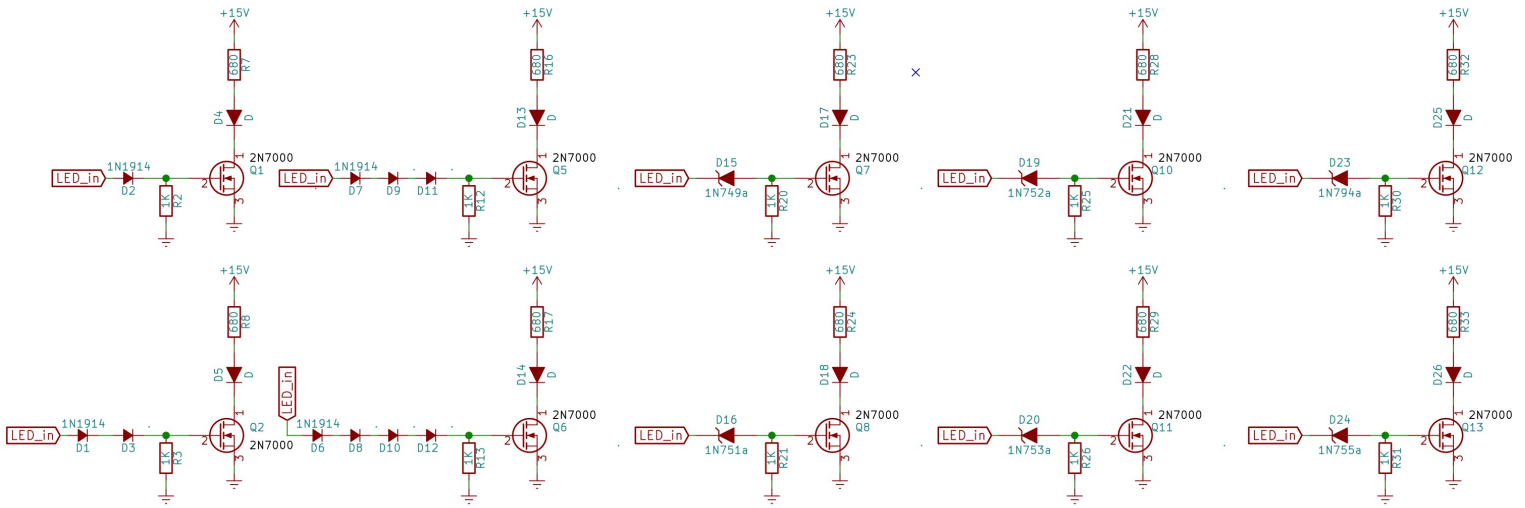
Figure 22. LED Bar Graph Circuit

Figure Y shows how 1n1914 diodes in series were used to create the first four LED trigger points, each 1V apart, but after that, zener diodes were used for simplicity. Resistors were selected to ensure that the current through the diodes was enough to operate in the correct regions of their respective curves. The top side resistor was used to current limit the LED when the MOSFET is driven on.
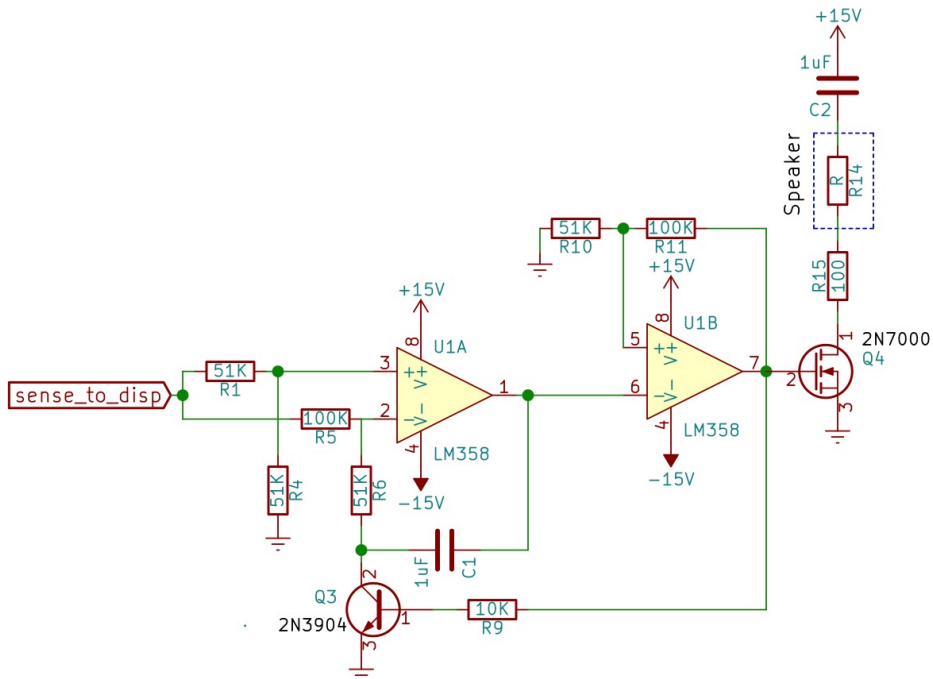
Figure 23. Ammeter Speaker Drive

The original 0 to 10V signal was also fed into a voltage controlled oscillator to create an audible frequency for feedback to the user. The VCO used two op-amps, as shown in Figure Z. When the N-channel BJT is turned on, current flows through the divider into the N-channel BJT. To maintain the voltage on the inverting input of the op-amp, the op-amp begins to drive the voltage across the capacitor higher. When the BJT is turned off, current flows from the capacitor and discharges it. Therefore the output voltage from the first op-amp drops. The result is a triangle waveform that was fed into the second op-amp stage, which acts like a Schmitt trigger. The output of this stage is a square wave. As the voltage rises on the input to the first op amp the frequency increases on the output as it supplies more current to the capacitor, charging more quickly. This output signal is sent to a single low side N-channel MOSFET driver which pulses a speaker for audible feedback.

IV. Challenges and Lessons Learned

Multiple debugging and design challenges were surmounted in completing this project at every stage in signal generation and processing. The most notable of these are discussed below.

One recurring problem is the mixing of analog and power circuits. Large current pulled or pushed through the ground can result in an offset to the ground, which can disturb the signal processing blocks. This happened when the signal chains was integrated with the display circuitry. Placing the two system's power rails in parallel instead of series resolved this specific case.

Another recurring problem resulted from placing blocking capacitors in series with high impedance nodes, a resistor must be tied in parallel to ground to ensure that the filter works. This caused occasional problems in DC removal in the system's chain.

One pitfall to avoid is ineffectively pushing the core into saturation. This can be avoided by observing the drive signal across the drive coil. If the signal is an unaltered square wave than the core is not saturated. Instead the voltage should drop to zero before and after rising edges, because during saturation the inductance is approximately zero. If the core is not being driven into saturation the number of coils must be decreased, or the permeability must be increased.

A challenge to the bar graph design is picking the correct diodes for the correct voltage drops. Limited selection can make this difficult, and switching to

Zener's after a point can make the design smaller. In addition variations in the 2N7000 V-threshold can cause undesired variance in the voltage steps between LEDs turning on. To prevent this 2n7000s were selected and checked for very similar characteristics on the lab meter. This makes repeatability difficult. In the future it would be wise to use a package that had more predictable values. Overall the variations did not create extremely noticeable change in results (variation by .1V or so), so depending on desired specs this may be acceptable. For the application of a visual display this was reasonable.

One worthy design change for the future would be to produce a more efficient driver for the speaker, simplicity was desired as it was not the focus of this project to produce an extremely energy efficient system, but the 100 ohm ceramic resistor quickly rose to an uncomfortable temperature. In the future it would be preferable to use a push-pull amplifier as was used in prior labs to drive the speaker.

V. Conclusion

The fluxgate magnetometer system designed in this project was able to resolve the magnitude and direction of signals produced by external magnetic fields. The design took advantage of multiple analog circuitry techniques including, but not limited to signal generation, resonant tank filtration, and phase demodulation. The result is an accurate and robust system for a wide array of applications such as ammeters, permanent magnet detectors, and magnetic theremins. In future iterations the design would lend itself to a 3 axis expansion via printed circuit boards. Active current feedback could also be employed in order an even higher precision magnetic field sensor.

VI. Acknowledgements

Williams, Jason Yang, Mary Caulfield, and the rest of the 6.101 staff for your great help as we completed our final project.

VII.References

[1] http://www.imperial.ac.uk/space-and-atmospheric-physics/research/areas/space-magnetometer-laboratory/space-instrumentation-research/magnetometers/fluxgate-magnetometers/
[2] http://www.analog.com/media/en/training-seminars/tutorials/MT-202.pdf